Tellus (1998), 50B, 34–50
Printed in UK – all rights reserved

TELLUS
ISSN 0280–6509

Tropospheric ozone depletion in polar regions
A comparison of observations in the Arctic and Antarctic

By S. WESSEL[1]*, S. AOKI[2], P. WINKLER[3], R. WELLER[4], A. HERBER[1], H. GERNANDT[1] and O. SCHREMS[4], [1]*Alfred-Wegener-Institute of Polar and Marine Research, Research Department Potsdam, Potsdam, Germany,* [2]*Centre of Atmospheric and Oceanic Studies, Tohoku University, Sendai, Japan,* [3]*Deutscher Wetterdienst, Hohenpeissenberg, Germany,* [4]*Alfred-Wegener-Institute of Polar and Marine Research, Bremerhaven, Germany*

(Manuscript received 15 January 1997; in final form 1 September 1997)

ABSTRACT

The dynamics of tropospheric ozone variations in the Arctic (Ny-Ålesund, Spitsbergen, 79°N, 12°E) and in Antarctica (Neumayer-Station, 70°S, 8°W) were investigated for the period January 1993 to June 1994. Continuous surface ozone measurements, vertical profiles of tropospheric ozone by ECC-sondes, meteorological parameters, trajectories as well as ice charts were available for analysis. Information about the origins of the advected air masses were derived from 5-days back-trajectory analyses. Seven tropospheric ozone minima were observed at Ny-Ålesund in the period from March to June 1994, during which the surface ozone mixing ratios decreased from typical background concentrations around 40 ppbv to values between 1 ppbv and 17 ppbv (1 ppbv O_3 corresponds to one part of O_3 in 10^9 parts of ambient air by volume). Four surface ozone minima were detected in August and September 1993 at Neumayer-Station with absolute ozone mixing ratios between 8 ppbv and 14 ppbv throughout the minima. At both measuring stations, the ozone minima were detected during polar spring. They covered periods between 1 and 4 days (Arctic) and 1 and 2 days (Antarctica), respectively. Furthermore, it was found that in both polar regions, the ozone depletion events were confined to the planetary boundary layer with a capping temperature inversion at the upper limit of the ozone poor air mass. Inside this ozone- poor layer, a stable stratification was obvious. Back-trajectory analyses revealed that the ozone-depleted air masses were transported across the marine, ice-covered regions of the central Arctic and the South Atlantic Ocean. These comparable observations in both polar regions suggest a similar ozone destruction mechanism which is responsible for an efficient ozone decay. Nevertheless, distinct differences could be found regarding the vertical structure of the ozone depleted layers. In the Arctic, the ozone-poor layer developed from the surface up to a temperature inversion, whereas in the Antarctic, elevated ozone-depleted air masses due to the influence of catabatic surface winds, were observed.

1. Introduction

It has been found that the Arctic spring is characterised by a pronounced variability of surface ozone concentrations, accompanied by sudden strong ozone depletion events. During these non-periodical depletion events, the surface ozone mixing ratios decreased from around 40 ppbv to values close to the detection limit of 2 ppbv within a few hours (Barrie et al., 1988; Oltmans et al., 1989). This phenomenon could be observed at several Arctic sites like Barrow, Alaska (71°N, 156°W) (Oltmans et al., 1989) or Alert, Canada (82°N, 62°W) (Barrie et al., 1988) where it was first noticed during spring 1985 (Bottenheim et al., 1986). Continuous surface ozone

* Corresponding author.

measurements at Ny-Ålesund, Spitsbergen (79°N, 12°E), carried out since 1988 by the Norwegian Institute for Air Research (NILU, Kjeller) and since 1992 by the National Institute of Polar Research (NIPR, Tokyo), also showed similar ozone depletion events during springtime (Solberg et al., 1996; Wessel et al., 1997).

Coinciding with the strong decrease of surface ozone, an increase of particulate and gaseous bromine compounds could be observed (Barrie et al., 1988). Based on this anti-correlation between surface ozone and bromine compounds a catalytic photochemical ozone destruction mechanism, including reactive bromine, was proposed (Barrie et al., 1988). The primary source of ozone depleting bromine compounds is not yet clarified. There are some indications pointing to biogenic brominated organic compounds like bromoform, released by macro algae (Barrie et al., 1988), or seasalt aerosols which can liberate reactive inorganic bromine by heterogeneous reactions with nitric oxides (Finlayson-Pitts et al., 1990), HSO_5^- or HO_2-radicals (Mozurkewich, 1995) and by photoinduced conversion involving dissolved organic materials or transition metals (McConnell et al., 1992). Beside these primary sources of reactive bromine, a regeneration of nonreactive bromine reservoir substances by catalytic processes in the gas phase and on aerosol or ice surfaces is necessary to explain the observed ozone destruction (Tang and McConnell, 1996; LeBras and Platt, 1995; Fan and Jacob, 1992). The influence of anthropogenic pollutants like sulphate aerosols, which can act as a potential surface for heterogeneous reactions (Fan and Jacob, 1992) is not yet clarified.

In addition to photochemical reactions which are responsible for the destruction of ozone, dynamic processes, influencing the ozone depleted air mass, are also of great importance for the observed surface ozone destruction during polar spring. Measurements of the vertical distribution of tropospheric ozone during ozone minima by tethersondes (Anlauf et al., 1994) and ozone sondes (Solberg et al., 1996; Wessel et al., 1997) showed a vertical extension of ozone depleted air masses of typically several hundred meters. In general the upper limit of the ozone poor layer was defined by free temperature inversions. Trajectories pointed towards ice-covered regions of the Arctic Ocean as a marine source of the ozone depleted air masses (Anlauf et al., 1994).

For Antarctica, surface ozone measurements at the Japanese Syowa Station (69°S, 39°E) and the German Neumayer-Station (70°S, 8°W) indicated comparable low ozone events as they were observed in the Arctic (Murayama et al., 1992; Wyputta, 1994).

The topic of our research activities was to study the dynamics of tropospheric ozone distributions in the Arctic (Ny-Ålesund, Spitsbergen) as well as in Antarctica at the Neumayer-Station during the transition from polar night to polar day. The crucial point of our analysis are detailed case studies for typical tropospheric ozone minima observed in the Arctic and in the Antarctic, followed by a more general comparison of both regions considering previous studies of other groups. Emphasis will be laid on the dynamical processes during the tropospheric ozone minima.

2. Instrumentation and data acquisition

The Arctic observation site is located in Ny-Ålesund, Spitsbergen (79°N, 12°E). The measurements described below were conducted at two locations, the Japanese station "Rabben" which is approximately 2 km south-east of the village Ny-Ålesund at 40 m above sea level (a.s.l.) and the German Koldewey-Station, located in Ny-Ålesund 11 m a.s.l.

At the Koldewey-Station, ozone sondes were launched usually once a week and up to two times a day when tropospheric ozone minima could be observed. ECC- (electrochemical concentration cell) sondes were used together with modified RS80 radiosondes (both Vaisala) on TOTEX TA 1200 balloons. The ECC-sondes were prepared according to the detailed instructions given by Komhyr (1986). After launch the ECC-current, which is proportional to the ambient ozone partial pressure times the rate of the air flow, was measured continuously. The dependence of the ECC-current from the electrolyte concentration is negligible: Doubling the KI concentration results in a signal enhancement of 5% (Komhyr, 1986). Simultaneously, the meteorological data air temperature, pressure, relative humidity, wind velocity and wind-direction were measured by an attached RS80 radiosonde. The data were transmitted to a

DigiCORA MW11 receiver (Vaisala) installed in the ground station. The ascent velocity of the ozone sondes was around 5 m/s. Together with the inherent time constant of the ECC-sonde of approximately 20 s an effective height resolution of about 100 m was achieved. At the Japanese station "Rabben" surface ozone mixing ratios were measured continuously by means of an ozone analyser based on UV-absorption (Dasibi, Model 1006-AHJ). The ozone analyser is calibrated once a year at the National Institute of Environmental Studies (NIES, Tsukuba, Japan) by a reference UV-spectrometer equipped with an optical cell of one meter pathlength. With this ozone analyser O_3 mixing ratios up to 200 ppbv can be measured with an instrumental precision of ± 1 ppbv and an absolute detection limit of 1 ppbv.

Neumayer-Station (the German research station in Antarctica) is located 42 m a.s.l. at 70°S, 8°W on the Ekstrøm Ice Shelf in 5 km distance to the Atka Bay. The surrounding is flat and snow covered with a gentle slope upwards to the south. ECC-sondes were started regularly once a week. The types of the ECC and radiosondes and the ground instrumentation was identical to that at Ny-Ålesund. Surface ozone mixing ratios were detected continuously with a wet-chemical ozone analyser, described in detail by Attmanspacher (1971). With this ozone analyser ozone mixing ratios in the range of 0–100 ppbv could be detected with a precision of 1–3%. Meteorological data in 2 and 10 m height for temperature, relative humidity, wind direction, wind speed and pressure were provided by the regular meteorological observations of the Alfred-Wegener-Institute. The 5-days-back-trajectories were calculated by the German Weather Service (DWD) based on 3-D wind fields. Input data were the horizontal wind components and the surface pressure. The vertical wind component is derived from divergences and convergences of the wind field resulting in subsidence and updraft of air masses. The trajectories were calculated with endpoints at the observational site every day at 0000 UTC. In this study we selected trajectories with endpoint levels corresponding to surface pressure, 950 hPa, 850 hPa and 700 hPa. It should be noted that the model is not able to calculate trajectories for regions north of 86°N and south of 86°S. Additionally for the southern hemisphere weather-charts were available for further analysis. These forecasting charts for the Japanese Antarctic station were calculated by the Japanese Meteorological Agency (JMA) using the JMA global model. We used the pressure maps at sea level, which were calculated two times a day at 0000 and 1200 UTC. The sea ice coverage of the Arctic Ocean and the South Atlantic Ocean was derived from ice charts from the National Ice Center (NIC), Boulder, Colorado and the National Snow and Ice Data Center, Boulder, Colorado. For convenience, in our analysis the date is given as decimal day of the year (Julian Day = JD, Table 1) and the time in UTC.

Table 1. *Climatological seasons and their corresponding Julian Days for the Arctic and Antarctica*

Season	Julian Day Arctic	Julian Day Antarctic
spring	60–151	244–334
summer	152–243	335–59
autumn	244–334	60–151
winter	335–59	152–243

3. Results

At both stations, the annual cycle of surface ozone mixing ratios was derived from hourly mean values by calculating the running means over 30 days. The result, together with the hourly mean ozone mixing ratios is shown in Fig. 1. For the Neumayer-Station a summer minimum of about 18 ± 3.5 ppbv can be observed in December. The seasonal maximum of about 36 ± 2 pbv was reached during the southern polar winter in July. In contrast to these observations the annual maximum at Ny-Ålesund was found to be in March, with slightly higher ozone mixing ratios of 40 ± 6 ppbv. The Arctic summer minimum in June shows mixing ratios of about 30 ± 8 ppbv. During the Arctic and Antarctic springtime, a strong variability of surface ozone mixing ratios were observed at both polar stations. To investigate these variations in more detail, the difference between hourly mean ozone mixing ratios and the annual mean cycle was calculated for the period of interest, i.e., for the Arctic from JD 16 to 166 and for the Antarctic from JD 200 to 350 (Fig. 2). At both sites strong negative deviations between the hourly mean values and the seasonal mean value are obvious, but they are smaller in the

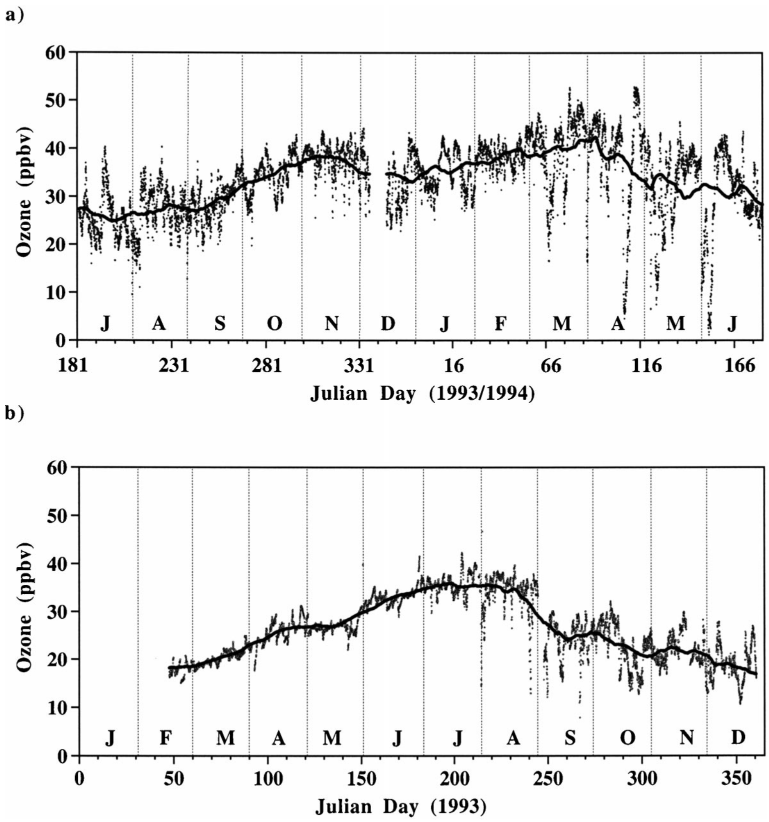

Fig. 1. Annual cycle of surface ozone mixing ratios for Ny-Ålesund, Spitsbergen, 1993/1994 (a) and for Neumayer-Station, Antarctic, 1993 (b). The solid line corresponds to the running mean over 30 days and the dots to hourly mean surface ozone mixing ratios.

Antarctic. For further analyses, it is useful to define the occurrence of a so-called tropospheric ozone minimum by some certain but, however, somewhat arbitrary criterions. For Ny-Ålesund a negative deviation of $\geqslant 22$ ppbv marks an Arctic tropospheric ozone minimum. Due to the fact that ozone depletion was not so pronounced at the Neumayer-Station a negative deviation $\geqslant 10$ ppbv over a period of more than 5 h was defined as an Antarctic tropospheric ozone minimum.

According to these definitions, seven tropospheric ozone minima were observed at Ny-Ålesund in spring 1994 and four at the Neumayer-Station in August and September 1993. The average and the minimum O_3 mixing ratios during each low ozone event and the difference of these values from the annual cycle are listed in Table 2. The tropospheric ozone depletion events covered periods from 1–4 days at Ny-Ålesund. They could be observed from March to June (Table 2). The duration of ozone depletion events at the Neumayer Station was approximately 1–2 days.

The vertical extensions of the ozone depleted air masses were measured by ozone soundings. At Ny-Ålesund eight ozone sondes were launched additionally to the routine soundings (two times a week) when the recorded surface ozone mixing ratios indicated the occurrence of ozone minimum. The vertical ozone distribution in the troposphere is presented in Fig. 3a. Unfortunately no ozone sondes were launched during the two ozone minima in March 1994 at JD 66–68 and JD 87–88. The ozone poor air mass was generally restricted to the planetary boundary layer (PBL) with a vertical extension of 0.5 km to 1 km. These layers

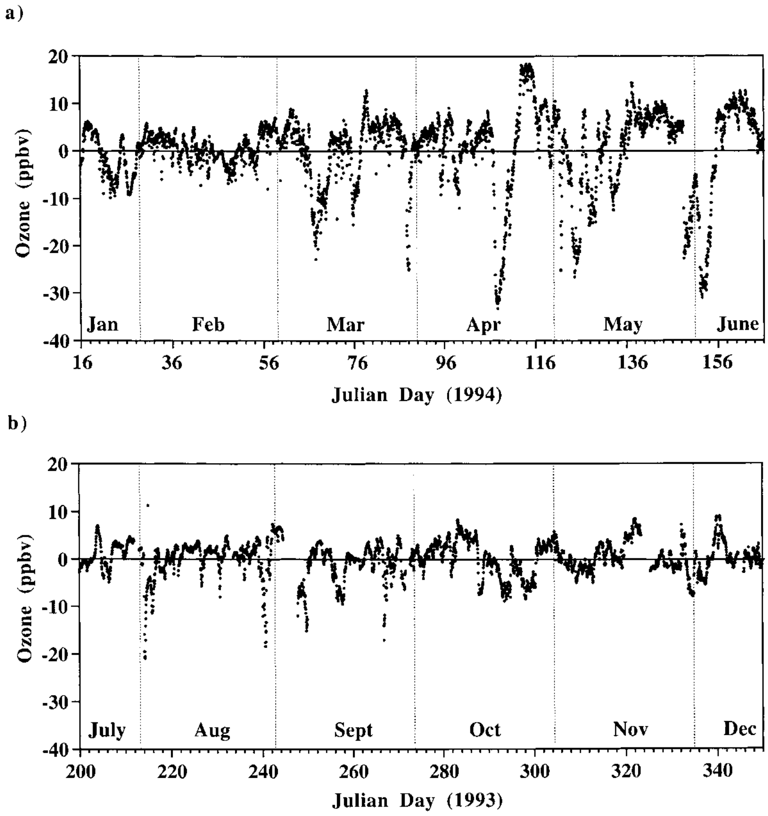

Fig. 2. Deviation of the hourly mean surface ozone mixing ratios and the seasonal mean value at Ny-Ålesund (a) and Neumayer-Station, Antarctica (b).

were characterised by a homogenous vertical distribution of low ozone mixing ratios. Above, ozone mixing ratios around 40–50 ppbv were observed.

At Neumayer-Station only three ozone minima could be detected by the routine ozone soundings (Fig. 3b). In contrast to the observations in the Arctic, the vertical structure of the ozone minima observed in August and September 1993 at Neumayer-Station showed higher ozone mixing ratios near the ground with an elevated ozone depleted layer above. This is particularly obvious at JD 267 and less pronounced, however, at JD 240 and JD 249. The vertical extension of the ozone depleted layers varied between 200 m (JD 240), 1600 m (JD 249) and 3000 m (JD 267). Above these confined ozone depleted layers a prompt increase to O_3 mixing ratios typical for the free troposphere of around 40 ppbv were found.

3.1. *Case studies: Arctic tropospheric ozone minima*

First, the tropospheric ozone minimum recorded between JD 106–110 will be discussed in detail. The temporal variations and vertical profiles of the ozone mixing ratio, temperature, relative humidity, and wind direction are shown in Figs. 4 and 5. Corresponding trajectories for this event, printed in isobaric levels, are presented in Fig. 6. The ozone minimum lasted 90 h. The O_3 concentration at the absolute minimum was around 5 ppbv, corresponding to a deviation of −36 ppbv with respect to the seasonal mean value. During the ozone minimum the temperature decreased from +3°C to −13°C, accompanied by a slight diurnal cycle. The temperature decrease started before the O_3 decay and continued when O_3 mixing ratios have already been recovered.

Table 2. *Average and minimum O_3 mixing ratios during each tropospheric ozone minimum and the difference of these values from the annual cycle*

Station	Julian day	Date	Average O_3 mixing ratio ± std. (ppbv) during the ozone minimum	Minimum ozone mixing ratio (ppbv) during the ozone minimum	Difference (ppbv) between the average O_3 mixing ratio of each ozone minimum and the annual cycle	Difference (ppbv) between the minimum O_3 value of each ozone minimum and the annual cycle
Neumayer	214–215	2–3 Aug. 1993	26.1 ± 7.6	14	−9.3	−21
Neumayer	239–241	27–29 Aug. 1993	24.8 ± 6.7	13	−6.5	−18
Neumayer	249–250	6–7 Sept. 1993	18.3 ± 4.3	12	−9.6	−15
Neumayer	266–268	23–25 Sept. 1993	22.7 ± 5.9	8	−2.2	−17
Ny-Ålesund	66–68	7–9 March 1994	28.4 ± 7.3	17	−11.0	−23
Ny-Ålesund	87–88	28–29 March 1994	30.6 ± 11.1	17	−11.0	−25
Ny-Ålesund	106–110	16–20 Apr. 1994	18.6 ± 11.6	5	−18.9	−36
Ny-Ålesund	121–122	1–2 May 1994	23.7 ± 9.9	6	−8.0	−25
Ny-Ålesund	123–126	3–6 May 1994	16.3 ± 6.1	7	−17.9	−27
Ny-Ålesund	148–151	28–31 May 1994	18.0 ± 5.5	9	−14.4	−22
Ny-Ålesund	151–155	31 May-4 Jun. 1994	12.8 ± 8.5	1	−19.4	−31

Both, the temperature and the relative humidity did not exhibit any significant correlations with the measured ozone mixing ratios. The ozone poor layer reached a vertical extension of 750 m. Within this layer the ozone mixing ratios increased from 5 ppbv at the surface to 17 ppbv at 750 m, corresponding to a positive gradient of 1.6 ppbv/100 m. Above 750 m the O_3 mixing ratios increased dramatically within a layer of 300 m from 17 ppbv to 41 ppbv, corresponding to a gradient of 7.8 ppbv/100 m. The vertical extension of the ozone depleted layer was limited by a temperature inversion (Fig. 5b). Within the temperature inversion a positive gradient of the potential temperature ($d\Theta/dz$) of 1 K/100 m was found. Thus, we assume that this inversion layer prevented downward-mixing of ozone rich air from the free troposphere. Inside the ozone poor layer the calculated potential temperature gradient of +0.5 K/100 m indicates a stable stratification. Below 750 m, the vertical profile of relative humidity showed values around 89 ± 4%. Inside the ozone poor layer the wind direction shifted from North (0°) at the surface to East-South-East (110°) at 750 m (Fig. 5d).

The abrupt change in the origin of the advected air masses is well documented by trajectory analyses (Fig. 6). Air masses with endpoint levels at ground and at 950 hPa, respectively, emanated from the the western part of the central Arctic and were transported from north of the Canadian Archipelago via north of Greenland to Spitsbergen. The air masses showed only marginal vertical movements (Fig. 6b). It is important to note, that the surface trajectory stayed close to the ground during the foregoing five days and thus was in contact with the ice covered Arctic Ocean. Unfortunately, due to numerical problems, the 950 hPa trajectory could be followed back for only two days. At the endpoint levels 850 hPa and 700 hPa, air masses with undisturbed O_3 mixing ratios advected from southern Greenland across the North Atlantic Ocean to Spitsbergen. This matched well to the local wind shear as recorded by radiosondes (Fig. 5d). At this day weather maps (Berliner Wetterkarte, DWD) showed a weak low located above Spitsbergen and a front approximately 100 km west of measuring site extending from north of the Fram Street to Jan Mayen.

Considering the remaining low ozone events observed at Ny-Ålesund, the following similarities are obvious. In all cases, the ozone depleted layers were restricted to the planetary boundary layer (PBL). Inside the ozone depleted layers the relative humidity was above 80% and the surface temperature generally decreased by 5–20 K. Except for JD 121, a capping temperature inver-

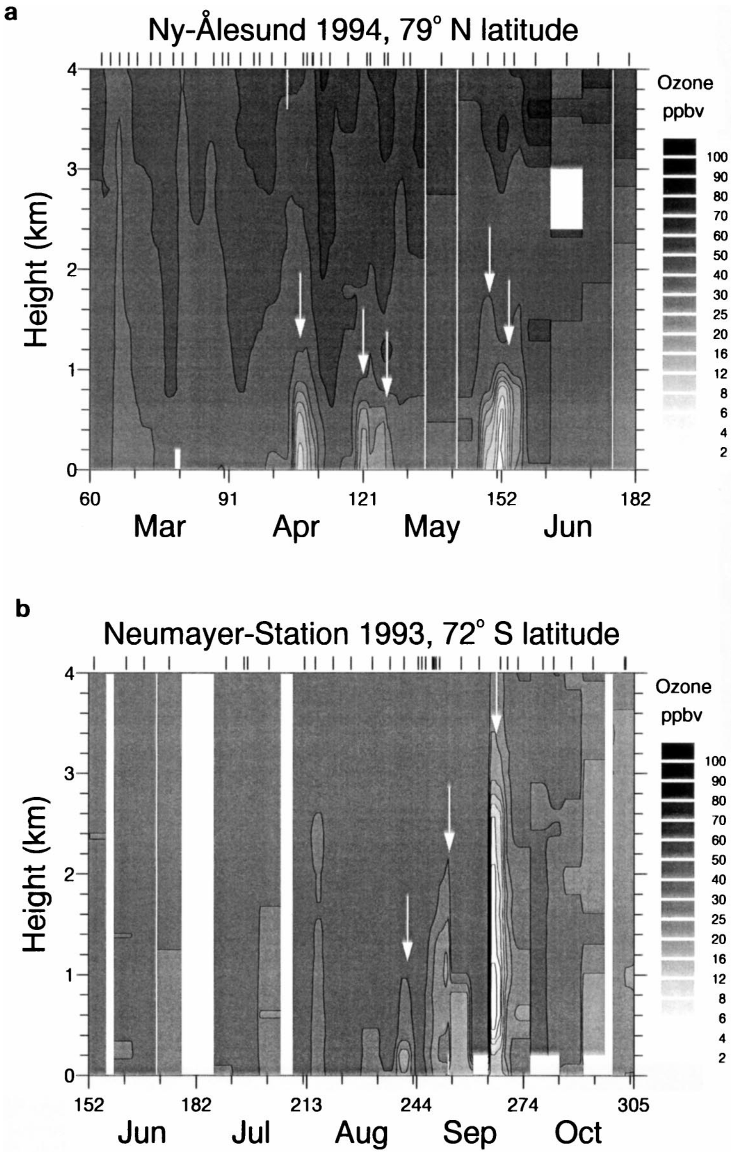

Fig. 3. Vertical stratification of tropospheric ozone mixing ratios from 0 to 4 km altitude Ny-Ålesund, for the period March–June 1994 (a) and Neumayer-Station, for the period June–October 1993 (b). The white arrows mark the ozone sondes started during tropospheric ozone minima. The ticks on the top of the figure mark the starts of the all ozone sondes.

sion coincided with the top of the ozone poor air mass during each ozone minimum. On JD 121, however, only an isothermal layer existed at the top of the ozone poor air mass. The vertical extension of the inversion layers varied between 100 m and 600 m with an average of 230 ± 130 m and the mean potential temperature gradient was around 0.3 ± 0.4 K/100 m. Except for JD 148 a stable stratification was found within the ozone depleted layers. The ozone-depleted air masses were generally advected from the western part of the central Arctic to the measuring site. In all

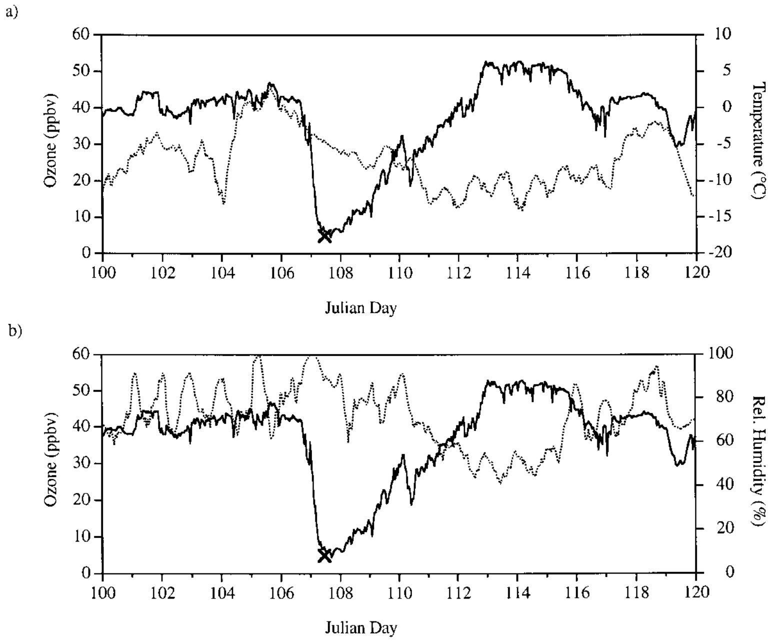

Fig. 4. Temporal development of surface ozone mixing ratios (solid line) and surface temperature (a), relative humidity (b), (dashed lines) at Ny-Ålesund, presented as hourly mean values. The cross marks the surface ozone mixing ratio measured by the ozone sonde at JD 107.

cases the air masses trajectories were exposed to sunlight. The total ice coverage in these source regions varied between 80% and 100%, as it could be derived from ice charts (National Snow and Ice Data Centre, Boulder, Colorado).

On the other hand, further analysis revealed that several cases could be observed, where similar meteorological conditions and a comparable air mass history were given, but no significant O_3 depletion occured (Wessel, 1996). So we conclude that the premises are necessary but not sufficient and a further non-periodical feature must exist to produce ozone minima.

3.2. *Case studies: Antarctic tropospheric ozone minima*

For the Neumayer-Station the ozone minimum at JD 266–268 was chosen for a detailed analysis. During this period, the temporal evolution of the surface ozone mixing ratios together with temperature and relative humidity is presented in Fig. 7. The ozone minimum covered a period of 45 h with minimum mixing ratios of 8 ppbv in the first phase and −17 ppbv deviation with respect to the running mean value. There is no obvious relation between the development of the surface ozone mixing ratios and surface temperature or relative humidity (Fig. 7). The surface temperature slightly increased during the second phase of the ozone minimum, whereas the relative humidity remained constant throughout the period. An ozone sonde was routinely launched during the second phase of the ozone minimum at JD 267 (Fig. 8). The surface ozone mixing ratio measured by the ozone sonde is marked by a cross in Fig. 7. Up from the ground, the ozone mixing ratios decreased to 2 ppbv at 500 m and increased again at 2600 m altitude. Background ozone mixing ratios as typical for the free troposphere were reached again at 3200 m altitude, giving a vertical extension of the elevated ozone poor layer of about 2100 m. At 2600 m, a pronounced temperature inversion defined the top of the ozone depleted layer. This inversion layer exhibited a vertical extension of 300 m with a gradient dT/dz of $+5.3$ K/100 m. Further a surface temperature inversion can be regarded as the lower limit of the ozone poor air

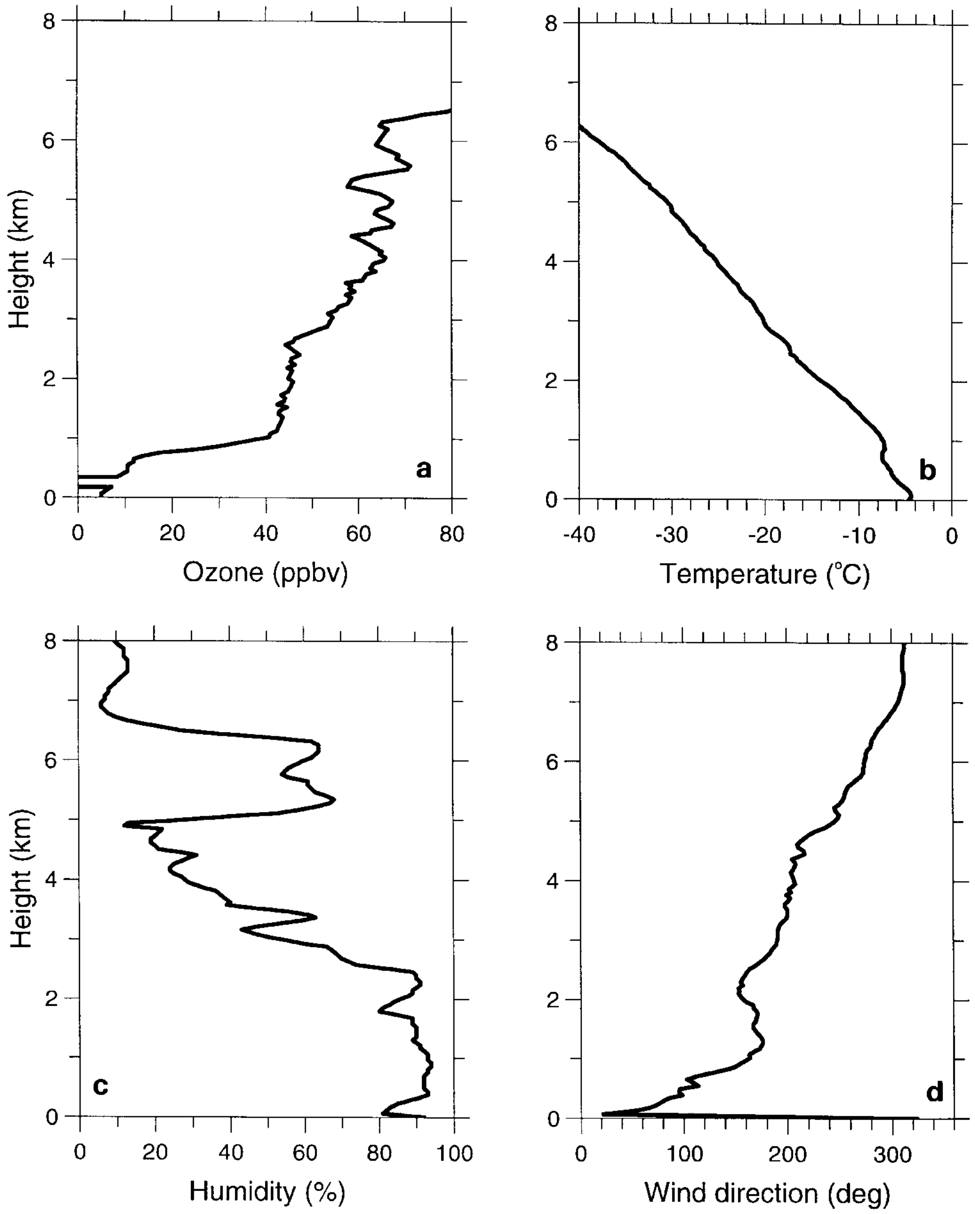

Fig. 5. Vertical profiles of ozone mixing ratios (a), temperature (b), relative humidity (c) and wind direction (d) at Ny-Ålesund, JD 107.

mass. The potential temperature within the ozone poor layer indicated a stable stratification with a gradient of +0.35 K/100 m, and the relative humidity was found to be around 60% within the entire boundary layer. The surface wind from the south (170°) shifted to east (90°) above 200 m altitude at the lower boundary of the ozone depleted layer. From these observations we conclude that cold katabatic surface winds from the continental ice shield lifted up warmer and less dense marine air masses with low ozone mixing ratios, so that the ozone minimum did not appear

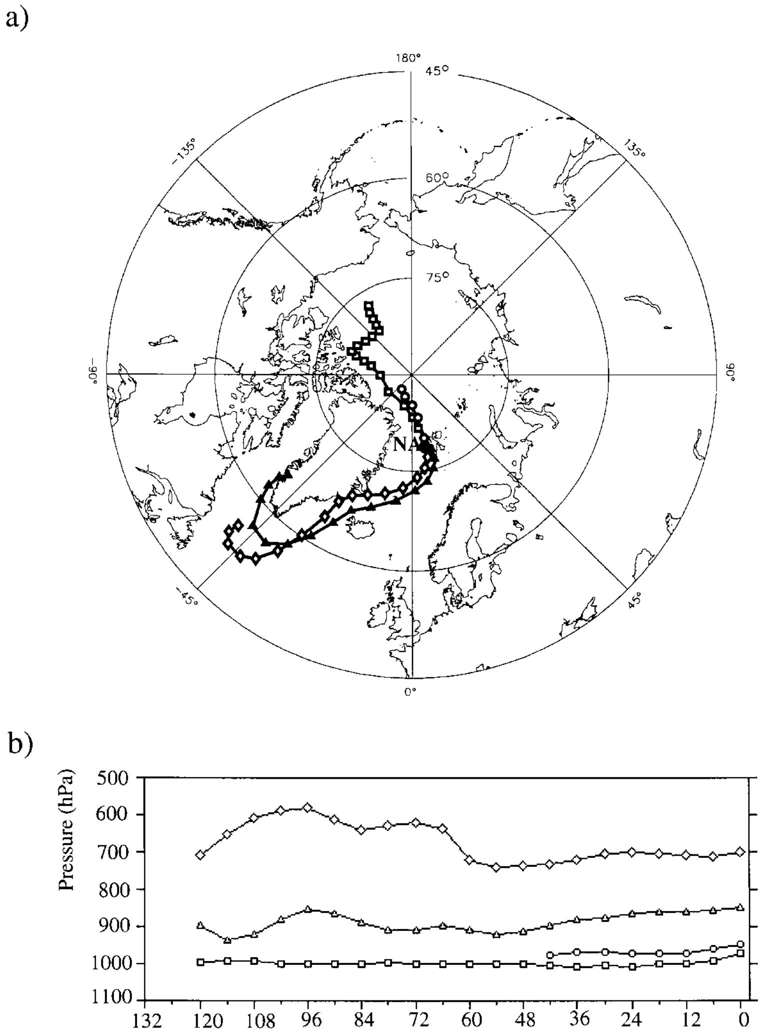

Fig. 6. (a) Trajectories which arrived in Ny-Ålesund at JD 107, corresponding to ground level (□), 950 hPa (○), 850 hPa (▲) and 700 hPa (◇). (b) Vertical movements of the air masses during the foregoing 120 hours. (□) Ground level, 1006.7 hPa (11 m), (○) 950 hPa (430 m), (△) 850 hPa (1300 m) and (◇) 700 hPa (2770 m).

at the ground but above 500 m. This is also confirmed by a trajectory analysis for JD 267 (Fig. 9). The surface and the 950 hPa trajectory, corresponding to higher ozone mixing ratios, showed an advection of continental air masses from the south-east. This air mass followed a sinking motion from the elevated Antarctic ice shield at 80°S (3700 m a.s.l., 500 hPa) to sea level within the foregoing 18 h, corresponding to a katabatic flow to the coast (Fig. 9b). Air masses above this katabatic flow with an endpoint level of 850 hPa originated from the South Atlantic Ocean and reached the station from north-eastern directions (Fig. 9a). This air parcel touched the ground above the South Atlantic 3.5 days before the lifting up to 850 hPa occured. At this time the surface of the South Atlantic Ocean was completely ice covered in this region, as it could be derived from ice charts (National Ice Center).

The ozone stratification throughout the min-

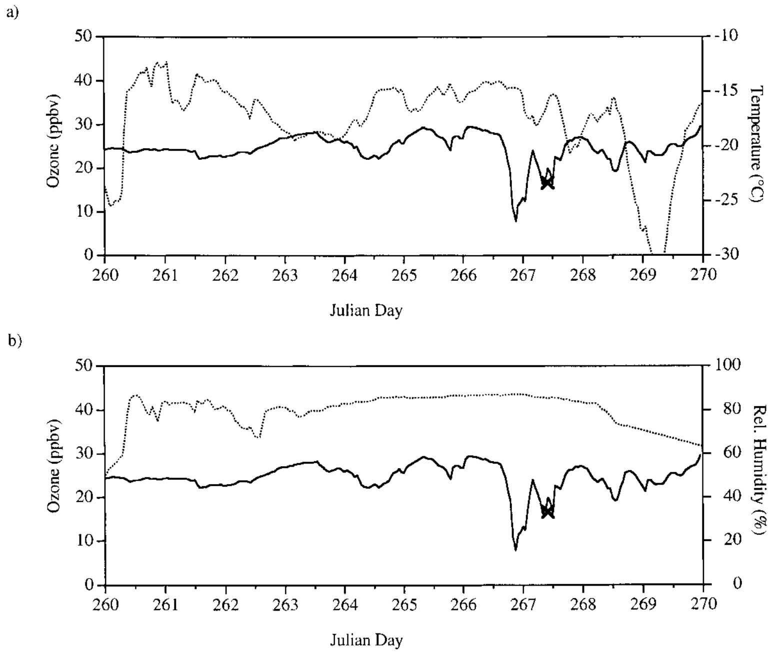

Fig. 7. Temporal course of surface ozone mixing ratios (solid line) and surface temperature (a), relative humidity (b), (dashed line) measured at Neumayer-Station for the period JD 260–270. The cross marks the surface ozone mixing ratio measured by the ozone sonde, started at JD 267.

imum at JD 249–250 showed an elevated ozone poor layer and higher ozone mixing ratios at the surface, comparable to the low ozone event at JD 266–268. A routine ozone sonde was launched during decreasing ozone mixing ratios at JD 249–250 (Fig. 3b). The ozone mixing ratios decayed from 19.5 ppbv at ground to 14 ppbv at 500 m altitude. Six hours later, comparable ozone mixing ratios of 12 ppbv could be observed at ground level (Fig. 10) possibly due to a change in the surface wind direction from south to east within this time period. The ozone depleted layer at JD 249 had a vertical extension of about 800 m. Here again, southerly katabatic surface winds reached the observation site and marine air masses with low O_3 mixing ratios, advected from eastern direction, were lifted up. Unfortunately, corresponding trajectories are not available to confirm this observation. The vertical structure of the low O_3 event during JD 239–241 resembled a typical arctic counterpart. The ozone depleted air mass was within a strong surface inversion reaching from the ground up to 1000 m height. Trajectories with endpoint levels at ground level and 950 hPa, corresponding to the ozone poor air, indicated a transport from the ice covered South Atlantic Ocean.

In summary, the available observational data from the Neumayer Station indicate that the ozone minima developed within the PBL. Generally, inside the ozone depleted layers high relative humidities between 70 and 95%, an increase of surface temperature between 2.5–9 K, and a stable stratification of the air were found. Except for the ozone minimum at JD 239–241, a pronounced temperature inversion coincided with the top of the ozone depleted layers.

Concerning the origin of the ozone depleted air masses we found that an advection from marine ice covered regions to the Neumayer-Station by polar cyclones took place. This could be derived from weather charts of the southern hemisphere (Japan Meteorological Agency) and by trajectory analyses, available for JD 240, JD 249 and JD

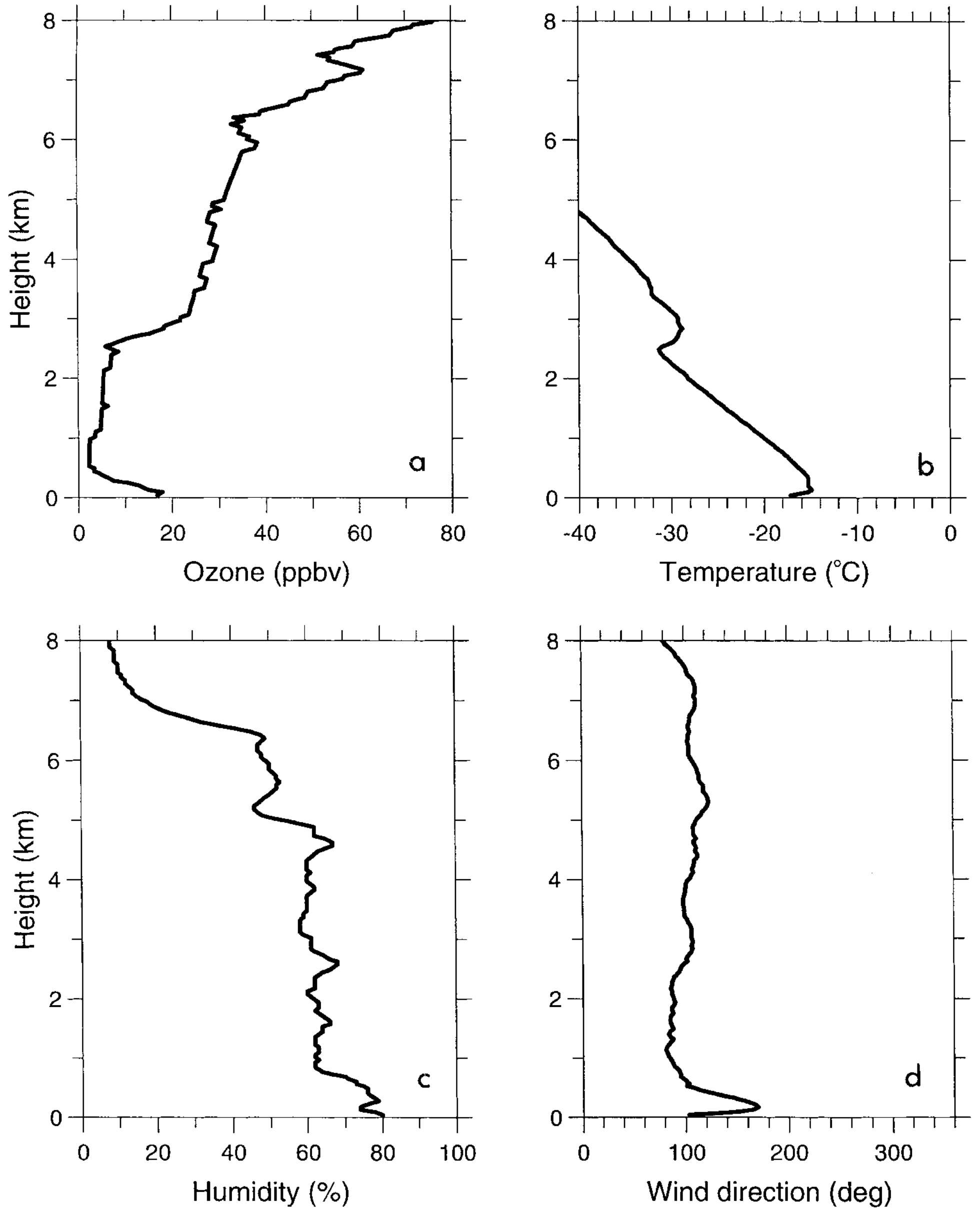

Fig. 8. Measured vertical profiles of the ozone mixing ratios (a), temperature (b), relative humidity (c), and wind direction (d) at Neumayer-Station, JD 267.

267. According to our observations every ozone depleted air mass originated from sunlit sea-ice covered regions. During the advection towards the measuring site they can be lifted up by continental katabatic winds.

A further analysis of additional cases with similar meteorological conditions but without ozone minima, as it was performed for the Arctic, was not carried out due to the small data record available. However, similar to the Arctic, we

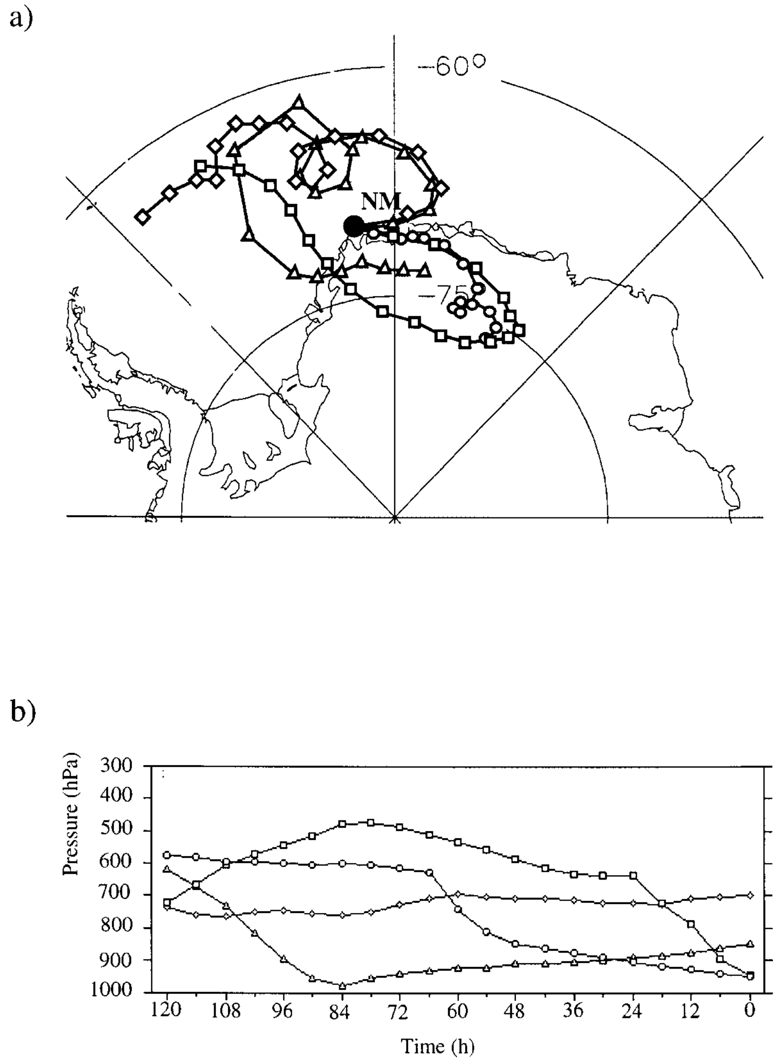

Fig. 9. (a) Trajectories which arrived Neumayer-Station at JD 267, ground level (□), 950 hPa (○), 850 hPa (△) and 700 hPa (◇). (b) Vertical movements of the air parcels. The trajectories started at 1200 UTC and arrived at Neumayer-Station 120 h later. (□) Ground level, 959.7 hPa (42 m), (○) 950 hPa (90 m), (△) 850 hPa (930 m) and (◇) 700 hPa (2360 m).

suggest that these characteristic meteorological features were necessary, but not sufficient for the occurrence of tropospheric O_3 depletion.

3.3. *Comparison of Arctic and Antarctic ozone minima*

Although observational data from Antarctica are rather limited, we present a comparison of the Arctic and Antarctic ozone minima based on our observations. At both polar stations the tropospheric ozone minima were restricted to the PBL, associated with high values of relative humidity. A capping temperature inversion generally defined the top of the ozone depleted air masses. Inside the ozone poor layers a stable stratification was found. Such air masses were moved across sea-ice covered marine regions of the Arctic and the

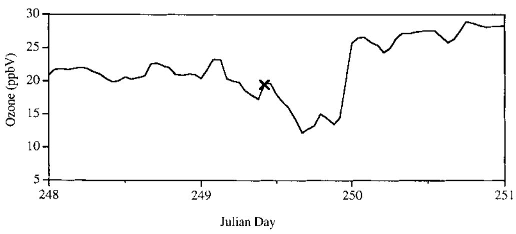

Fig. 10. Temporal course of surface ozone mixing ratios (hourly mean values) at Neumayer-Station for the period JD 248–251. The cross marks the surface ozone mixing ratio measured by the ozone sonde, launched at JD 249.

South Atlantic Ocean, respectively. In both polar regions, tropospheric ozone minima could exclusively be observed when the corresponding air masses were advected across sunlit sea-ice covered regions, supporting the idea that a photochemical liberation of ozone depleting compounds during late winter/springtime, as suggested by several authors (Barrie et al., 1988; McConnell et al., 1992; Hausmann and Platt 1994), seems to be essential for the ozone loss.

Comparing the vertical structure of the ozone depleted layers in the Arctic and Antarctic, some distinct differences were revealed: In the Arctic the ozone depleted layers included the entire boundary layer from the surface up to a temperature inversion. At the Neumayer-Station, however, due to the influence of katabatic surface winds, elevated ozone depleted air masses in connection with higher ozone mixing ratios at ground level seemed to be characteristic. Here, the ozone depleted layers were confined by temperature inversions at the bottom and at the top. In addition it should be noted that in Antarctica the observed tropospheric ozone minima occurred 1–2 months earlier in the year than in the Arctic.

4. Discussion

In a previous work, Wyputta (1994) presented the annual cycle of surface ozone mixing ratios at the Neumayer-Station based on hourly mean values in the years from 1982 to 1987. This six-years observation period revealed the seasonal occurrence of ozone minima during the month June-October with low ozone mixing ratios typically between 2 and 4 ppbv. Considering the seasonality, frequency and intensity of these ozone minima, our results are in agreement with this study. Sturges et al. (1993) reported on tropospheric ozone minima at McMurdo Station (77°S, 166°E). They measured surface ozone mixing ratios as low as 10 ppbv by ozone sondes. The same phenomenon was described by Murayama et al. (1992) for the coastal Syowa Station (69°S, 39°E). In contrast, low ozone events could never be detected at stations located in central Antarctica, like the Amundsen-Scott-Station at the South Pole (Schnell et al., 1991). So it is suggested that tropospheric ozone minima seem to be restricted to coastal and thus marine regions.

A similar pattern is obvious in the Arctic. During spring tropospheric ozone minima are typical at coastal sites like Ny-Ålesund, Barrow (Oltmans et al., 1989), Alert (Barrie et al., 1988), and Heiss-Island (Franz-Josef-Land, 80°N, 57°E) (Khattatov, personal communication). Due to the absence of pronounced katabatic wind patterns at these locations the minima reach down to the surface.

Concerning a possible ozone depletion mechanism, one has to consider that in contrast to Antartica the Arctic is proned to massive intrusions of anthropogenic emissions during polar night (Ottar, 1989; Worthy et al., 1994). In this context it should be noted that aerosol size distribution measurements, carried out during the field campaign in 1994 at Ny-Ålesund, revealed that the ozone poor air masses were associated with striking low particle number densities in the accumulation mode, especially in the size range of 0.09–1 μm diameter (Wessel et al., 1997). This confirms comparable observations at Alert during the Polar Sunrise Experiment (PSE, 1992, (Staebler et al., 1994)). Aerosols within this mode primarily consist of anthropogenic sulphate particles (d'Almeida, 1991), indicating that at least in these cases ozone depletion may have occurred without anthropogenic contamination being involved.

4.1. Horizontal and vertical distribution of the ozone minima

The characterisic similarities concerning the vertical structure of ozone depleted air masses are in general agreement with the investigations of other groups performed at Ny-Ålesund (Solberg et al., 1996), Alert (Anlauf et al., 1994), Sodankylä, Bear

Island and Ny-Ålesund (Taalas et al., 1993). At Alert O_3 depleted layers reached up to a temperature inversion at only 300–400 m height (Anlauf et al., 1994). This is much lower than the vertical extensions of ozone poor air masses reaching up to 1200 m at Ny-Ålesund and even up to 3200 m at the Neumayer-Station. Furtheron, at Neumayer-Station a surface temperature inversion coincided with the lower limit of the ozone poor air mass. An interesting phenomenon, which could not yet be observed at Arctic stations, was the influence of katabatic winds at Neumayer-Station, causing an elevation of the ozone depleted air masses. Moreover, up to now, this behaviour could neither be observed at the Syowa-Station (Aoki, 1995) nor at McMurdo (Sturges et al., 1993). Both stations are located at islands, where the continental katabatic wind is less pronounced. Neumayer-Station is directly located at the ice shelf where pronounced katabatic winds occur, so the detection of tropospheric ozone minima can not be completely observed in a surface ozone data record.

Beside the vertical structure of ozone depleted layers, their horizontal extension was estimated using local wind data and the duration of the ozone minimum. In this way, a horizontal extension of roughly 800 ± 300 km for the Arctic and 1000 ± 400 km for the Antarctic was derived. These values are comparable to calculations of Hausmann and Platt (1994). They estimated a horizontal extension of about 500 km for ozone depleted air parcels observed in Alert during the Polar Sunrise Experiment (PSE) 1992.

4.2. Source of the ozone-depleted air masses

A striking positive correlation was observed between the surface temperature and surface ozone during the PSE 1992 (Bottenheim et al., 1990). Solberg et al. (1996) generally observed decreasing temperatures during ozone minima at the Zeppelin-Station (Ny-Ålesund, 474 m a.s.l.) in their data record from 1989 to 1993. This is in agreement with our observations in 1994 at this site, whereas for the Neumayer-Station no general correlation could be established. In both regions, however, the relative humidity was high inside the ozone depleted layer, consistent with a marine origin of those air masses. In Antarctica ozone depleted air parcels were transported by marine cyclones, developing above the ice covered South Atlantic Ocean. These observations are confirmed by Yurganov (1990), who discovered a pronounced ozone minimum within a cyclone during a ship cruise through the pack ice of the Weddell Sea. However, ozone depletion did not necessarily occur in every marine cyclone (Wyputta, 1994; this study, JD 242). Trajectories, calculated for JD 242, point to the ice free South Atlantic Ocean around 55°S to be the source region of air masses with undisturbed O_3 mixing ratios. In this context, it is interesting to note that Yurganov (1990) found ozone depleted air exclusively inside the cold sector of the cyclone, corresponding to air masses from polar regions, but not inside the warm sector which corresponds to subpolar air.

Concerning the situation in the Arctic, Taalas et al. (1993) also found that air masses of remote marine origin exhibited low ozone mixing ratios. At JD 121, however, the ozone depleted air mass was advected across Greenland via the Greenland Sea to Spitsbergen. A similar case was observed by Hopper and Hart (1994) during the PSE 1992 at Alert. In contrast to our findings, they observed a high variability of the surface ozone mixing ratios during this event. Enhanced vertical mixing of the ozone poor boundary layer air with free tropospheric air masses, caused by the topography of Greenland may be the reason for this peculiarity (Hopper and Hart, 1994). Unfortunately, due to the short duration of the O_3 minimum at Spitsbergen during JD 121 a possible variability of the O_3 mixing ratios during this event is hard to detect. A missing variability would be consistent with the ice covered Greenland Sea west of Spitsbergen having been the source region of the ozone depletion and so the influence of the topography of Greenland would have been irrelevant.

5. Conclusions

Our analysis revealed several similar characteristic features of the tropospheric ozone depletions events at both stations, Ny-Ålesund in the Arctic and Neumayer Station in Antarctica. There are some indications supporting the idea that a comparable, if not the same mechanism, is responsible for the frequent O_3 decay in both polar regions: The observed ozone minima were generally associated with the advection of marine, polar air masses emanating above ice covered, sunlit regions. Low particle concentrations in the accumulation mode, as observed in the Arctic inside ozone poor air masses, indicated that ozone depleted air masses coincide with low concentrations of anthropogenic pollutants. This is consistent with the observation of low ozone events in the pristine Antarctic and points to a natural process causing tropospheric ozone depletion in polar regions. Due to the fact that in Antarctica the sea-ice covered regions are at much lower latitudes and thus hit by solar radiation much earlier compared to the Arctic, ozone minima seem to occure 1–2 months earlier in the year.

On the other hand, one has to be aware that the observational data from Antarctica are rather limited, making a general comparison problematic. Furtheron, we emphasize that the role of anthropogenic pollutants on tropospheric ozone depletion during the arctic springtime is not clarified. It is well-established that in the Arctic catalytic ozone destruction by reactive bromine compounds takes place and for both polar regions natural bromine precursors like brominated organic compounds and sea-salt aerosols are available. However, the crucial point is the mechanism liberating reactive bromine from these reservoir substances. It is hard to imagine that this mechanism will not be at least influenced or even provoked by the high burden of anthropogenic trace gases and aerosols during arctic winter and early spring which has no counterpart in Antarctica. However, a natural process seems to play a certain role even in the Arctic, but may be influenced by the impact of pollutants. For Antarctica further work has to proof that bromine catalysed ozone destruction is responsible for the surface ozone depletions, as indicated by the results of Sturges et al. (1993).

6. Acknowledgements

We would like to thank the German Weather Service (DWD) for the calculation of air mass trajectories which were used in this work. For the cooperation and the surface ozone data we would like to express our gratitude to the National Institute of Polar Research (NIPR), Tokyo. We also thank all overwinters of the Neumayer- and Koldewey-Station for the conduction of the measurements and Dr. P. von der Gathen and M. Rex for helpful discussions. The snow and ice data for the Arctic were obtained from the National Snow and Ice Data Center, Boulder, Colorado (NSIDC) as well as the snow and ice data for the Antarctic from the National Ice Center, Boulder Colorado (NIC). We also thank the Japan Meteorological Agency (JMA) for providing us the weather charts of the southern hemisphere.

REFERENCES

Anlauf, K. G., Mickle, R. E. and Trivett, N. B. A. 1994. Measurement of ozone during Polar Sunrise Experiment 1992. *J. Geophys. Res.* **99D**, 25 345–25 354.

Aoki, S. 1995. A study of tropospheric ozone depletion in the Antarctic. *Report for a Grant-in-Aid for scientific research from the Japanese Ministery of Education, Science and Culture* (Monbougho) Grant No. 05640482, Tokyo, available at the National Institute of Polar Research (NIPR), Tokyo.

Attmannspacher, W. 1971. Ein einfaches naßchemisches Gerät mit geringer Trägheit zur Messung des bodennahen Ozons in der Atmosphäre. *Meteorologische Rundschau* **24**, 183–188.

Barrie, L. A., Bottenheim, J. W., Schnell, R. C., Crutzen, P. J. and Rasmussen, R. A. 1988. Ozone destruction and photochemical reactions at polar sunrise in the lower Arctic atmosphere. *Nature* **334**, 138–141.

Bottenheim, J. W., Gallant, A. G. and Brice, K. A. 1986. Measurements of NO_y species and O_3 at 82° latitude. *Geophys. Res. Lett.* **13**, 113–116.

Bottenheim, J. W., Barrie, L. A., Atlas, E., Heidt, L. E., Niki, H., Rasmussen, R. A. and Shepson, P. B. 1990. Depletion of lower tropospheric ozone during the Arctic spring: The Polar Sunrise Experiment 1988. *J. Geophys. Res.* **95D**, 18 555–18 568.

d'Almeida, G. A., Koepke, P. and Shettle, E. P. 1991. In: *Atmospheric aerosols. Global climatology and radiative characteristics.* A Deepak Publishing, Virginia, p. 48.

Fan, S.-M. and Jacob, D. J. 1992. Surface ozone depletion in Arctic spring sustained by bromine reactions on aerosols. *Nature* **359**, 522–524.

Finlayson-Pitts, B. J., Livingston, F. E. and Berko, H. N. 1990. Ozone destruction and bromine photochemistry at ground level in the Arctic spring. *Nature* **343**, 622–625.

Hausmann, M. and Platt, U. 1994. Spectroscopic measurement of bromine oxide and ozone in the high Arctic during Polar Sunrise Experiment 1992. *J. Geophys. Res.* **99D**, 25 399–25 415.

Hopper, J. F. and Hart, W. 1994. Meteorological aspects of the 1992 Polar Sunrise Experiment. *J. Geophys. Res.* **99D**, 25 315–25 328.

Komhyr, W. D. 1986. *Operations-Handbook. Ozone measurements to 40 km altitude with model 4A electrochemical concentration cell (ECC) ozonesondes.* NOAA Technical Memorandum, ERL ARL-149, Nat. Oceanic and Atmos. Admin., Washington, D. C.

LeBras, G. and Platt, U. 1995. A possible mechanism for combined chlorine and bromine catalysed destruction of tropospheric ozone in the Arctic. *Geophys. Res. Lett.* **22**, 599–602.

McConnell, J. C., Henderson, G. S., Barrie, L., Bottenheim, J., Niki, H., Langford, C. H. and Templeton E. M. J. 1992. Photochemical bromine production implicated in arctic boundary layer ozone depletion. *Nature* **355**, 150–152.

Mozurkewich, M. 1995. Mechanisms for the release of halogens from sea salt particles by free radical reactions. *J. Geophys. Res.* **100D**, 14 199–14 208.

Murayama, S., Nakazawa, T., Tanaka, M., Aoki, S. and Kawaguchi, S. 1992. Variations of tropospheric ozone concentration over Syowa Station, Antarctica. *Tellus* **44B**, 262–272.

Oltmans, S. J., Komhyr, W. D., Franchois, P. R. and Matthews, W. A. 1989. Tropospheric ozone: Variations from surface and ECC ozonesonde observations. In: *Ozone in the atmosphere, Proceedings of the Quadrennial Ozone Symposium 1988 and Tropospheric Ozone Workshop*, (eds. R. D. Bojkov, P. Fabian). A Deepak Publishing, Hampton Virginia, 539–543.

Ottar, B. 1989. Arctic air pollution: A Norwegian perspective. *Atmos. Environ.* **23**, 2349–2356.

Schnell, R. C., Liu, S. C., Oltmans, S. J., Stone, R. S., Hofmann, D. J., Dutton, E. G., Deshler, T., Sturges, W. T., Harder, J. W., Sewell, S. D., Trainer, M. and Harris, J. M. 1991. Decrease of summer tropospheric ozone concentrations in Antarctica. *Nature* **351**, 726–729.

Solberg, S., Schmidbauer, N., Semb, A. and Stordal, F. 1996. Boundary-layer ozone depletion as seen in the Norwegian Arctic in spring. *J. Atmos. Chem.* **23**, 301–332.

Staebler, R. M., den Hartog, G., Georgi, B. and Düsterdiek, T. 1994. Aerosol size distributions in the Arctic haze during Polar Sunrise Experiment 1992. *J. Geophys. Res.* **99D**, 25 429–25 438.

Sturges, W. T., Sullivan, C. W., Schnell, R. C., Heidt, L. E. and Pollock, W. H. 1993. Bromoalkane production by Antarctic ice algae. *Tellus* **45B**, 120–126.

Taalas, P., Kyrö, E., Supperi, A., Tafuri, V. and Ginzburg, M. 1993. Vertical distribution of tropospheric ozone in Antarctica and in the European Arctic. *Tellus* **45B**, 106–119.

Tang, T. and McConnell, J. C. 1996. Autocatalytic release of bromine from Arctic snow pack during Polar Sunrise. *Geophys. Res. Lett.* **23**, 2633–2636.

Wessel, S. 1996. *Troposphärische Ozonvariationen in Polarregionen.* PhD Thesis, University of Bremen, Germany, September 1996.

Wessel, S., Aoki, S., Weller, R., Herber, A., Gernandt, H. and Schrems, O. 1997. Aerosol and ozone observations in the polar troposphere at Spitsbergen in spring 1994. *Atmos. Res.* **44**, 175–189.

Worthy, D. E. J., Trivett, N. B. A., Hopper, J. F., Bottenheim, J. W. and Levin, I. 1994. Analysis of long-range transport events at Alert, Northwest Territories, during the Polar Sunrise Experiment. *J. Geophys. Res.* **99D**, 25329–25344.

Wyputta, U. 1994. *Untersuchungen zum Spurenstofftransport in die Antarktis anhand von Messungen an der Georg-von-Neumayer-Station.* PhD Thesis, Hamburg. Berichte aus dem Zentrum für Meeres-und Klimaforschung Reihe A, No. 15.

Yurganov, L. N. 1990. Surface layer ozone above the Weddell Sea during the Antarctic spring. *Antarctic Science* **2**, 169–174.